

## THE FIRST DEFINITIVE BINARY ORBIT DETERMINED WITH THE *HUBBLE SPACE TELESCOPE* FINE GUIDANCE SENSORS: WOLF 1062 (GLIESE 748)<sup>1</sup>

OTTO G. FRANZ,<sup>2</sup> TODD J. HENRY,<sup>3</sup> LAWRENCE H. WASSERMAN,<sup>2</sup> G. FRITZ BENEDICT,<sup>4</sup> PHILIP A. IANNA,<sup>5</sup>  
J. DAVY KIRKPATRICK,<sup>6</sup> DONALD W. MCCARTHY, JR.,<sup>7</sup> ARTHUR J. BRADLEY,<sup>8</sup> RAYNOR L. DUNCOMBE,<sup>9</sup>  
LAURENCE W. FREDRICK,<sup>5</sup> PAUL D. HEMENWAY,<sup>10</sup> WILLIAM H. JEFFERYS,<sup>11</sup> BARBARA E. MCARTHUR,<sup>4</sup>  
EDMUND P. NELAN,<sup>12</sup> PETER J. SHELUS,<sup>4</sup> DARRELL B. STORY,<sup>13</sup>  
WILLIAM F. VAN ALTENA,<sup>14</sup> AND ARTHUR L. WHIPPLE<sup>8</sup>

Received 1998 March 17; revised 1998 May 12

### ABSTRACT

The M dwarf binary, Wolf 1062 (Gliese 748), has been observed with the *Hubble Space Telescope* (*HST*) Fine Guidance Sensor 3 in the transfer function scan mode to determine the apparent orbit. This is the first orbit defined fully and exclusively with *HST*, and is the most accurate definitive orbit for any resolved, noneclipsing system. The orbital period is  $2.4490 \pm 0.0119$  yr and the semimajor axis is  $0''.1470 \pm 0''.0007$ —both quantities are now known to better than 1%. Using the weighted mean of seven parallax measurements and these *HST* data, we find the system mass to be  $0.543 \pm 0.031 M_{\odot}$ , where the error of 6% is due almost entirely to the parallax error. An estimated fractional mass from the infrared brightness ratio and infrared mass-luminosity relation yields a mass for the primary of  $0.37 M_{\odot}$ , and the secondary falls in the regime of very low mass stars, with a mass of only  $0.17 M_{\odot}$ .

*Key words:* astrometry — binaries: close — stars: fundamental parameters — stars: individual (Wolf 1062) — stars: low-mass, brown dwarfs

### 1. INTRODUCTION

The M dwarf binary Wolf 1062 (Gliese 748;  $V = 11.12$ , R.A.  $19^{\text{h}}12^{\text{m}}14^{\text{s}}.5$ , decl.  $+02^{\circ}53'12''$  [J2000.0]) is one target in an observational program to refine the mass-luminosity relation (MLR) for the most populous members of the Galaxy, the red dwarfs. The review article by Liebert & Probst (1987) provided the first comprehensive evaluation of the MLR for red dwarfs, with special emphasis on those with masses less than  $0.20 M_{\odot}$  (spectral type  $\sim M4$  V). Empirically determined MLRs near the end of the main sequence have improved considerably during the past decade, primarily as a result of infrared speckle techniques.

Henry & McCarthy (1993) used infrared speckle measurements in the *J*, *H*, and *K* passbands to define the first robust near-infrared MLRs for these very low mass objects, including 10 objects with masses confidently known to be less than  $0.20 M_{\odot}$ . However, their MLR at optical wavelengths, specifically the *V* bandpass, required estimating  $M_V$  from infrared absolute magnitudes and an empirical *V*–*K* relation, because few of the faint binaries had been resolved at optical wavelengths. In addition, the errors in the masses were still significant, usually 10%–30%. Only when masses are known to 5% can the important effects of age and metallicity on the lower main sequence be evaluated, and the transition region between stars and brown dwarfs near  $0.08 M_{\odot}$  be explored effectively.

To improve the MLR at the end of the main sequence, an aggressive observational campaign has been initiated to determine masses to better than 5%. To meet this rigorous goal, only binary systems that are the most promising for high-precision mass determinations have been selected. Such binaries must be nearby to allow accurate parallax measurements and to present relatively large orbital separations. To finish the project in a reasonable amount of time, they must also have relatively short orbital periods. Finally, to investigate the MLR to the end of the stellar main sequence, they must contain at least one component of very low mass. We have developed the “20-20-20 Sample” to meet these criteria. The sample includes systems within 20 pc that have periods shorter than 20 yr and that contain at least one component with a mass less than 20% that of the Sun. This sample of a few dozen systems is being observed to map the orbits to high accuracy with the *Hubble Space Telescope* (*HST*) Fine Guidance Sensor 3 (FGS3), as well as in ground-based infrared speckle imaging and radial velocity programs.

Here we report on the target observed most extensively with *HST* FGS3 in this program, Wolf 1062, and provide the first definitive binary orbit determined by *HST*. It is now an opportune time to examine this binary in detail,

<sup>1</sup> Based on observations with the NASA/ESA Hubble Space Telescope, obtained at the Space Telescope Science Institute, which is operated by the Association of Universities for Research in Astronomy, Inc., under NASA contract NAS 5-26555.

<sup>2</sup> Lowell Observatory, 1400 West Mars Hill Road, Flagstaff, AZ 86001.

<sup>3</sup> Harvard-Smithsonian Center for Astrophysics, 60 Garden Street, Cambridge, MA 02138-1516.

<sup>4</sup> McDonald Observatory, University of Texas at Austin, Austin, TX 78712-1083.

<sup>5</sup> Department of Astronomy, University of Virginia, P.O. Box 3818, Charlottesville, VA 22903-0818.

<sup>6</sup> Infrared Processing and Analysis Center, Mail Stop 100-22, California Institute of Technology, Pasadena, CA 91125.

<sup>7</sup> Steward Observatory, University of Arizona, 933 North Cherry Avenue, Tucson, AZ 85721.

<sup>8</sup> AlliedSignal Aerospace Company, 7474 Greenway Center Drive, Suite 200, Greenbelt, MD 20770.

<sup>9</sup> Department of Aerospace Engineering, University of Texas at Austin, Austin, TX 78712.

<sup>10</sup> Department of Physics, University of Rhode Island, 2 Lippitt Road, Kingston, RI 02881.

<sup>11</sup> Department of Astronomy, University of Texas at Austin, Austin, TX 78712-1083.

<sup>12</sup> Space Telescope Science Institute, 3700 San Martin Drive, Baltimore, MD 21218.

<sup>13</sup> Jackson & Tull, Chartered Engineers, 7375 Executive Place, Lanham, MD 20706.

<sup>14</sup> Department of Astronomy, Yale University, P.O. Box 208101, New Haven, CT 06520-8101.

because it has completed 98% of a full orbit under the *HST* program, and because no additional observations were made until after the second *HST* servicing mission (SMOV2), when instrumental recalibrations may be required.

## 2. TARGET: THE WOLF 1062 SYSTEM

Basic photometric and spectroscopic data for the Wolf 1062 system are given in Table 1. The system was first discussed as an astrometric binary by Harrington (1977) and Lippincott (1977). They found periods of 2.3 and 2.45 yr, respectively, and the semimajor axis of the photocentric orbit to be  $\sim 0''.03$ . Because the companion remained unseen, however, only the orbit of the system's photocenter was known, and the mass estimates for the components had to be considered coarse. Harrington's orbit, combined with assumptions about the mass of the primary, resulted in mass estimates of  $0.34 M_{\odot}$  and  $0.15 M_{\odot}$  for the components. Similarly, Lippincott found mass ranges of  $0.22$ – $0.32 M_{\odot}$  and  $0.06$ – $0.13 M_{\odot}$  for the pair, indicating that the secondary might in fact be substellar. Although accurate masses eluded the researchers at the time, the secondary was clearly of low mass, and worthy of continued effort.

A decade later, one-dimensional infrared speckle scanning observations confirmed that the system was, indeed, a binary with a magnitude difference of  $\Delta K$  ( $2.2 \mu\text{m}$ ) =  $1.4 \pm 0.1$  mag (McCarthy 1986). The separation measured by infrared speckle was compared with that predicted by the astrometric orbits at the epoch of resolution to yield the scale of the apparent orbit. This allowed the first mass estimates for the components:  $0.4 \pm 0.2 M_{\odot}$  and  $0.10 \pm 0.04 M_{\odot}$  (Liebert & Probst 1987).

Nearly another decade passed before Wolf 1062 was first resolved at visible wavelengths by Franz et al. (1994) using *HST* FGS3. A second observation 6 weeks later confirmed the detection. By late 1995, four additional observations had been obtained, extending coverage to nearly half of the orbit, and a first "visual" orbit with  $P = 2.423 \pm 0.055$  yr and  $a = 0''.1462 \pm 0''.0007$  was derived (Franz et al. 1995). Since then, eight additional observations have been made of the system, and the *HST* data now yield a definitive apparent orbit solution. In the following sections we illustrate the

power of *HST* FGS3 as an astrometric instrument, present the apparent orbit for Wolf 1062, and compare the components to other stars in the MLR of Henry & McCarthy (1993).

## 3. DATA: OBSERVATIONS AND REDUCTION

### 3.1. Advantages of Observing with *HST* FGS3

Four characteristics of a high-resolution ( $\leq 1''$ ) observing technique must be considered when attempting to resolve a target binary: the source brightness limit, the resolving capability, the astrometric accuracy, and the magnitude difference between the components that can be observed. Although all four parameters are interdependent, we provide current "best case" guidelines for each characteristic here separately in order to illustrate the efficacy of *HST* FGS3 as an astrometric instrument when compared with optical and infrared speckle efforts.

For objects as faint as Wolf 1062 ( $V = 11.12$ ), *HST* FGS3 observations provide astrometric accuracy currently unachievable with ground-based techniques. *HST* FGS3 is accurate to 1–3 mas at a resolution limit of 15 mas for magnitude differences less than 2 mag. It can effectively observe targets to at least  $V = 15$ . At component separations greater than  $\sim 200$  mas, it can bridge brightness differences of at least  $\Delta V = 4$  mag, as demonstrated by the detection of Gliese 623B (Franz et al. 1994). Optical speckle techniques result in measurements accurate to a few mas for a resolution limit near 30 mas on a 4 m telescope. However, these techniques are limited to relatively bright targets with  $V \leq 11$ , and detect companions only moderately fainter than the primaries searched, typically to  $\Delta V = 3$  (Hartkopf 1992). Although infrared speckle programs have not provided the same high-accuracy astrometry (typical errors are 10–20 mas with a resolution limit of 110 mas at  $K$  on a 4 m telescope), they have historically probed fainter targets than optical speckle, to  $K = 10$  (or  $V \sim 19$ ), and can reach fainter companions, to  $\Delta K = 5$  (corresponding to  $\Delta V \sim 8$ ), than any other high-resolution method (Henry & McCarthy 1993). Clearly, each of the three techniques has its advantages. Future developments in ground-based interferometers should improve the accuracy of the astrometric measurements and provide better resolution, but will still be limited to relatively bright targets and moderate magnitude differences. *HST* FGS3 is the only high-resolution instrument currently available that (1) can provide high-precision astrometry for very close binaries, (2) allows relatively faint targets to be observed, and (3) can bridge at least moderately large magnitude differences between the components in a binary system.

### 3.2. Observations with *HST* FGS3

Observations of the Wolf 1062 system have been made during  $2\frac{1}{2}$  yr under *HST* observing programs GTO 5174 (Cycle 4: two observations), GO 6047 (Cycle 5: nine observations), and GO 6566 (Cycle 6: three observations prior to SMOV2). *HST* FGS3, the "astrometry" FGS, has been used in the transfer function scan mode (hereafter, TRANS) to measure the component separation, position angle, and brightness difference through filter F583W at each epoch. Details on observing with FGS3 in TRANS mode can be found in Franz et al. (1992) and in the FGS Instrument Handbook (Holfeltz 1996). The number of TRANS scans per visit was 32 to 43 and the scan length

TABLE 1  
AVAILABLE DATA FOR WOLF 1062

Parameter	Value <sup>a</sup>	Reference
$B_{\text{Johnson}}$ .....	12.63	1
$V_{\text{Johnson}}$ .....	11.12	1
$R_{\text{Kron}}$ .....	9.80	1
$I_{\text{Kron}}$ .....	8.64	1
$J_{\text{CIT}}$ .....	7.08	2
$H_{\text{CIT}}$ .....	6.55	2
$K_{\text{CIT}}$ .....	6.31	2
$L_{\text{CIT}}$ .....	6.05	2
Spectral type <sup>b</sup> .....	M3.5 V	3
$\Delta K$ .....	$1.4 \pm 0.1$	4
$\tau_{\text{abs}}$ (arcsec) .....	$0.0998 \pm 0.0024$	5
	$0.09856 \pm 0.00266$	6

<sup>a</sup> Photometric and spectroscopic data include both components.

<sup>b</sup> On KHM system (Kirkpatrick, Henry, & McCarthy 1991).

REFERENCES.—(1) Weis 1996; (2) Leggett 1992; (3) this paper; (4) McCarthy 1986; (5) van Altena et al. 1995; (6) ESA 1997.

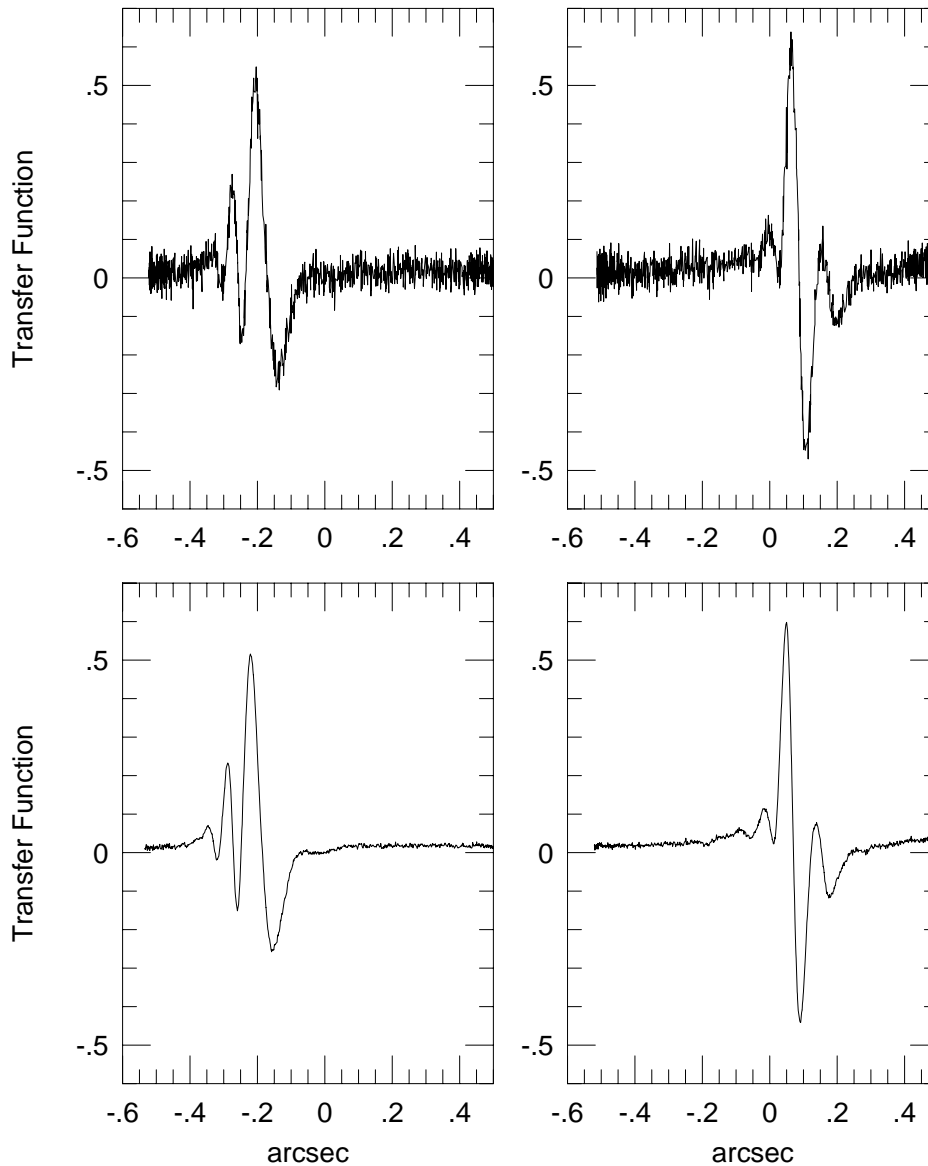


FIG. 1.—Example of *HST* FGS3 TRANS observations of Wolf 1062, obtained 1995 day 209 (1995.5712) near minimum component separation. *Top*: scan 16 (of 32 scans) along the FGS *X* (*left*) and *Y* (*right*) axes. *Bottom*: the corresponding transfer functions by co-addition of all 32 scans.

0".80 to 1".20 along each scan axis. *HST* FGS3 position mode (POS) observations have also been made relative to a set of four reference stars, so that the proper motion, the parallax, and the mass ratio of the system can ultimately be determined (Benedict et al. 1994).

### 3.3. Data Reduction and Analysis

For each visit to Wolf 1062, the individual TRANS scans in FGS3 *X*, *Y* were “dejittered,” inspected for data quality, cross-correlated, and co-added. The best available *X*, *Y* transfer functions for a single star of appropriate *B*–*V* color were used to analyze the co-added binary star scans. The concept and details of the analysis procedure may be found in Franz et al. (1991). This reduction and analysis procedure is illustrated in Figures 1 and 2 for the Wolf 1062 data set of 1995 day 209 (1995.5712), with the components cleanly resolvable on both axes by the algorithm (though not by visual inspection), and near their smallest observed separation.

## 4. RESULTS: ORBIT, MASSES, AND THE MASS-LUMINOSITY RELATION

### 4.1. Astrometry and the Apparent Orbit

In Table 2 we list the epochs, measured separations ( $\rho_{\text{obs}}$ ), position angles ( $\theta_{\text{obs}}$ ), and magnitude differences  $\Delta m$  through filter F583W for the 14 *HST* FGS3 observations. Our analysis normally yields, for each epoch, independent magnitude difference values along with the effective separations in FGS *X* and *Y*. For nine epochs, at which the two effective separations differed by a factor of 2 or more, we listed in Table 2 the magnitude difference associated with the larger projected separation. For the remaining cases we used either the average of the two independent values or the sole value that could be determined. The tabulated positions are based upon the observed FGS3 *X*, *Y* measurements, adjusted for an instrumental effect that was first identified and empirically characterized by Whipple (1996, private communication) with the use of an extensive series

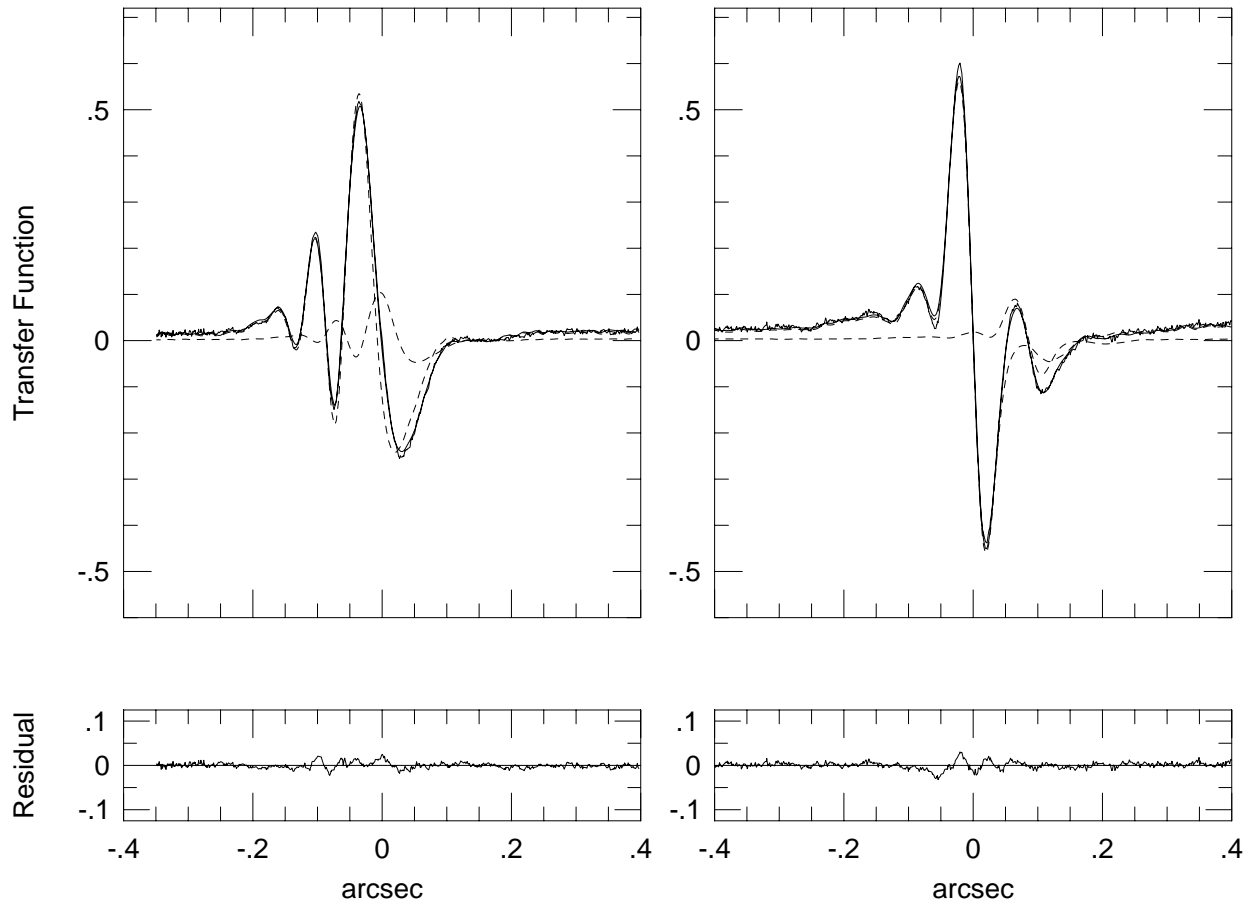


FIG. 2.—Analysis of the 1995.5712 observation of Wolf 1062. The computed (*smoothed solid line*) curves in *X* (*left*) and *Y* (*right*) represent best-fitting linear superpositions of two single-star functions (*dashed curves*) to the co-added scans. The relative displacements of the single-star curves are  $0''.0329 \pm 0''.0003$  and  $0''.0862 \pm 0''.0002$  along FGS *X* and *Y*, respectively. They yield separation and position angle, while the relative amplitudes of the single-star curves yield a magnitude difference for the binary components. The systematic trends in the curve-fitting residuals (*bottom panels*) are caused by imperfect single-star calibrations. Their effect upon the astrometry and photometry of the Wolf 1062 components is negligible.

TABLE 2  
HST FGS3 OBSERVATIONS OF WOLF 1062

DATE	$\rho_{\text{obs}}$	$\theta_{\text{obs}}^{\text{a}}$	$\Delta m$	ORBIT I: 14 POINTS			ORBIT II: 12 POINTS		
				$\Delta\rho$	$\Delta\theta$	$\rho\Delta\theta$	$\Delta\rho$	$\Delta\theta$	$\rho\Delta\theta$
1994.4989 .....	0.2073	346.45	1.77	0.0007	-0.24	-0.0009	0.0007	-0.27	-0.0010
1994.6176 .....	0.2022	341.56	1.82	-0.0012	0.33	0.0012	-0.0013	0.29	0.0010
1995.5712 .....	0.0920	239.41	1.99	0.0036	2.40	0.0037	0.0033	2.38	0.0037
1995.6535 .....	0.0876	215.97	1.95	0.0005	-0.22	-0.0003	-0.0001	-0.45	-0.0007
1995.6915 .....	0.0877	205.55	1.94	0.0007	-0.93	-0.0014	0.0000	-1.30	-0.0020
1995.7607 .....	0.0881	188.29	1.93	0.0024	-0.31	-0.0005	0.0016	-0.98	-0.0015
1995.8576 <sup>b</sup> .....	0.0769	158.56	1.96	0.0000	-2.03	-0.0027	(-0.0009)	(-3.35)	(-0.0046)
1996.2239 .....	0.1117	035.74	1.74	-0.0012	0.11	0.0002	-0.0002	0.19	0.0004
1996.3020 .....	0.1315	024.89	1.84	-0.0016	-0.69	-0.0016	-0.0010	-0.48	-0.0011
1996.4046 .....	0.1574	015.90	1.72	0.0011	-0.18	-0.0005	0.0013	0.10	0.0003
1996.4487 .....	0.1641	012.14	1.72	-0.0008	-0.63	-0.0018	-0.0007	-0.34	-0.0010
1996.7347 .....	0.2004	355.57	1.87	-0.0001	-0.95	-0.0033	-0.0003	-0.65	-0.0023
1996.7564 <sup>b</sup> .....	0.2020	356.56	1.85	0.0001	1.08	0.0038	(0.0000)	(1.38)	(0.0048)
1996.9051 .....	0.2059	349.26	1.82	-0.0008	0.64	0.0023	-0.0008	0.93	0.0034
Mean <sup>c</sup> .....			$1.85 \pm 0.09^{\text{d}}$	0.0011	0.77	0.0017	0.0009	0.70	0.0015
N .....			14	14	14	14	12	12	12

<sup>a</sup> Equinox J2000.0

<sup>b</sup> The pair was unresolved along the FGS3 *X*-axis;  $\rho_{\text{obs}}$  and  $\theta_{\text{obs}}$  are based upon an assumed  $\Delta X = 0$ .

<sup>c</sup> Mean of the absolute values for all astrometric data.

<sup>d</sup> Standard deviation of individual  $\Delta m$  values.

of FGS3 data for L726-8, a wide (FGS3-covered separation range 1".7 to 1".2), low-mass binary. The effect was subsequently interpreted by R. R. Crout (1996, private communication) as the result of rotation of the Koester Prisms in FGS3 from nominal alignment.

The current empirical formulation of the effect in FGS3 coordinates is a nonorthogonal transformation with different scale factors in  $X$  and  $Y$ . If the primary component of a binary is at position  $(X, Y)$  and the secondary at an offset  $(dX, dY)$ , then the adjusted position of the secondary  $(X', Y')$  becomes

$$X' = X + dX', \quad Y' = Y + dY', \quad (1)$$

where

$$dX' = A dX + B dY, \quad dY' = C dX + D dY, \quad (2)$$

with

$$A = 1.02621, \quad B = 0.00279, \quad C = 0.00199, \quad D = 0.99049. \quad (3)$$

All separations, position angles, and derived orbit solutions presented here include these adjustments. Orbit solutions for Wolf 1062 based upon positions with and without the adjustment have shown that it has a negligible effect upon the orbital elements and no effect upon the resulting total mass of the system.

At two epochs, 1995.8576 and 1996.7564, the separation vector of the binary components was nearly aligned with the FGS3  $Y$ -axis because of the instantaneous roll angle of

*HST*, making the binary unresolvable along the  $X$ -axis. Because at two other epochs the pair was resolved and reliably measured in  $X$  at 19 and 15 mas, respectively, the  $X$  separation at the two epochs noted above was certainly less than 15 mas. Given the moderate brightness ratio in this system, *detection* of the secondary would have been achieved to 10 mas. Because in both cases the residuals of the transfer function analysis in  $X$  show no evidence of a secondary, the separation along that axis must have been less than 10 mas. We have adopted an  $X$  separation of zero in deriving the tabulated component positions for these two epochs.

The elements for two orbital solutions are given in Table 3. Orbit I includes all 14 points. Orbit II has been generated without the two epochs at which the companion was not resolved along the  $X$  axis. The differences ( $O - C$ ) between the observed values and those computed from the orbital fits for the separations ( $\Delta\rho$ ) and for the position angles ( $\Delta\theta$ ) and the arc-equivalents ( $\rho \Delta\theta$ ) are given in Table 2 for both orbital solutions. There is little difference between the mean absolute  $O - C$  values for the two orbital fits, listed in the next-to-last line of Table 2. This supports the assumption of zero separation along the  $X$  axis in the two cases noted. The solutions in Table 3 are nearly identical. We consider Orbit I the definitive orbital solution because it includes all of the observational data.

The Orbit I solution is plotted in Figure 3. Solid points indicate the 12 epochs for which resolution was achieved along both the  $X$  and  $Y$  axes. The two open points are those for which the separation along the  $X$ -axis was assumed to

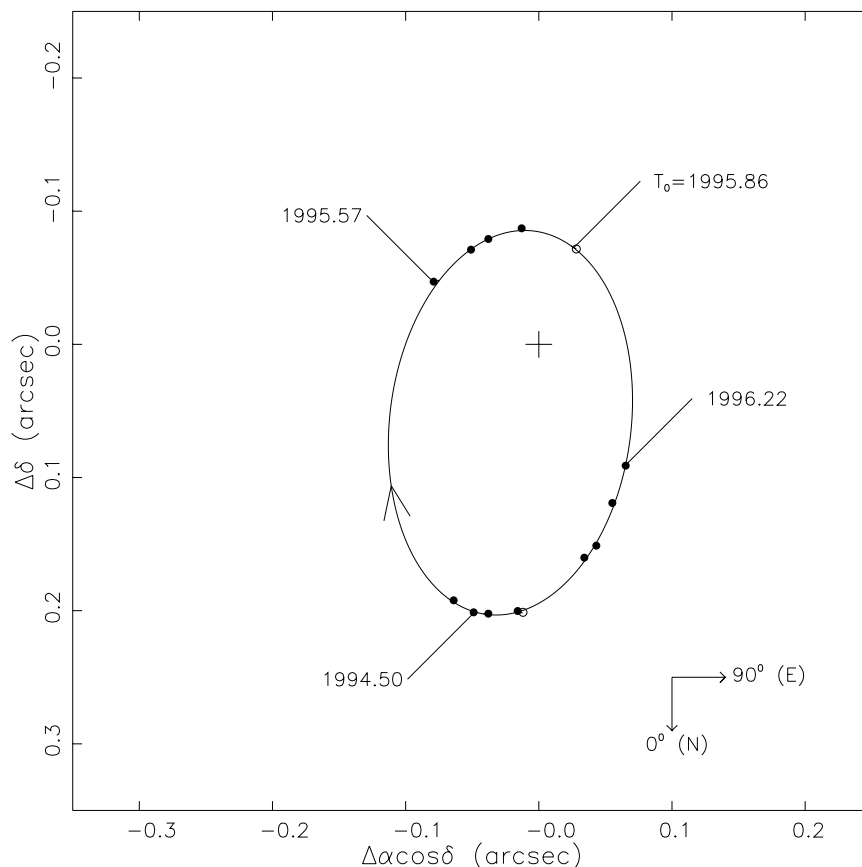


FIG. 3.—*HST* FGS3 measurements of Wolf 1062AB (Table 2) and the orbital path predicted by the derived elements (Table 3, Orbit I) are shown. Three epochs of observation and the time of periastron  $T_0$  are labelled. Residual vectors for all data points are plotted, but are smaller than the points themselves.

TABLE 3  
ORBITAL ELEMENTS, ABSOLUTE MAGNITUDES, AND MASSES FOR  
WOLF 1062

Parameter	Orbit I: 14 points	Orbit II: 12 points
$P$ (yr).....	$2.4490 \pm 0.0119$	$2.4417 \pm 0.0105$
$P$ (days).....	$894.48 \pm 4.34$	$891.81 \pm 3.84$
$T_0$ .....	$1995.8579 \pm 0.0039$	$1995.8632 \pm 0.0051$
$a$ (arcsec).....	$0.1470 \pm 0.0007$	$0.1475 \pm 0.0008$
$e$ .....	$0.4503 \pm 0.0042$	$0.4483 \pm 0.0045$
$i$ (deg).....	$133.05 \pm 0.80$	$132.52 \pm 0.82$
$\omega$ (deg).....	$25.20 \pm 1.21$	$25.89 \pm 1.12$
$\Omega$ (deg).....	$178.30 \pm 0.83$	$178.26 \pm 0.72$
$\pi_{\text{abs}}$ (arcsec).....	$0.09919 \pm 0.00180$	
$\Delta F583W$ .....	$1.85 \pm 0.09$	
$\Delta V$ .....	$1.82 \pm 0.09$	
$M_{VA}$ .....	$11.29 \pm 0.05$	
$M_{VB}$ .....	$13.11 \pm 0.09$	
$M_{KA}$ .....	$6.56 \pm 0.05$	
$M_{KB}$ .....	$7.96 \pm 0.09$	
Mass ( $M_{\odot}$ ):		
Total.....	$0.543 \pm 0.031$	$0.552 \pm 0.032$
A.....	$0.370 \pm 0.022$	$0.377 \pm 0.023$
B.....	$0.173 \pm 0.012$	$0.175 \pm 0.012$

be zero. Three epochs of observation and the time of periastron  $T_0$  (very near to one of the observations that was unresolved along the  $X$ -axis) are labelled. As listed near the bottom of Table 2, the mean absolute difference between the observed and computed separations is only 1.1 mas, and only  $0^{\circ}.77$  in the position angle. On Figure 3, residual vectors for all data points are drawn, but are smaller than the points. Perhaps it is even more impressive to realize that *the box illustrated is only  $0^{\circ}.6$  in size, so that "good" seeing from the ground would result in a stellar image the size of the entire figure.*

#### 4.2. Magnitude Difference

The mean value and standard error of the 14 measurements of the magnitude difference between Wolf 1062A and B through the F583W filter are 1.85 and 0.09 mag, respectively. To determine the magnitude difference in the  $V$  bandpass,  $\Delta V$ , rather than that measured,  $\Delta F583W$ , the transformation from F583W to  $V$  given in the FGS Instrument Handbook is used:

$$V = F583W + 20.060 - 0.164(B - V). \quad (4)$$

Simple algebra then yields

$$\Delta V = \Delta F583W + 0.164[(B - V)_A - (B - V)_B]. \quad (5)$$

Thus, the conversion of  $\Delta V$  to  $\Delta F583W$  is weakly dependent on the difference in the  $B - V$  color of the components in a binary.

To estimate the  $B - V$  colors for the components of Wolf 1062, we use the measured  $M_K$  values and a  $(B - V)$  versus  $M_K$  relation for red dwarfs developed from available photometric data. We confirm that the components of Wolf 1062 are red dwarfs, not white dwarfs, given their measured colors of  $F583W - K \approx 4.7$  and  $5.2$  for A and B, respectively, so this fit is an appropriate one to use. The stars selected for the relation (1) have  $B$ ,  $V$ , and  $K$  photometry in Leggett (1992) and/or Weis (1996), (2) have photometry uncontaminated by known nearby sources (close binaries eliminated), (3) are within 10 pc of the Sun, thereby having high-quality parallaxes, and (4) are on the main sequence (white dwarfs eliminated). Ninety-two stars satisfy these cri-

teria and yield a least-squares, third-order polynomial fit described by

$$B - V = +0.02184(M_K)^2 - 0.18541M_K + 1.82517 \\ (4.59 \leq M_K \leq 9.97). \quad (6)$$

From this relation, the  $M_K = 6.56 \pm 0.05$  of Wolf 1062A implies  $(B - V) = 1.549 \pm 0.005$ , whereas for Wolf 1062B, with  $M_K = 7.96 \pm 0.09$ ,  $(B - V) = 1.733 \pm 0.015$ . These errors are from those in the  $M_K$  values alone (discussed in § 4.3). The rms of the fit, due to age and metallicity differences among the 92 stars used, is 0.045 mag, and dominates the error in the  $(B - V)$  estimates. The color estimated for the primary, which dominates the light, is certainly consistent with the color of A and B combined,  $(B - V) = 1.51$  (identical values in both Leggett 1992 and Weis 1996).

The adjustment in  $\Delta F583W$  to obtain  $\Delta V$  (the second term in eq. [5]) is then computed to be  $-0.030 \pm 0.011$  mag, where the error includes contributions from uncertainties in the measured  $M_K$  values, the cosmic scatter in  $(B - V)$  for a given  $M_K$ , as well as the error,  $\pm 0.010$ , in the coefficient, 0.164, of equation (5). Finally, the magnitude difference in the  $V$  bandpass is found to be  $\Delta V = 1.82 \pm 0.09$ , its uncertainty dominated by the scatter among the 14 measurements of  $\Delta F583W$ .

#### 4.3. Masses

Four quantities are needed to determine the masses of components in a binary system: orbital period, semimajor axis of the apparent orbit, parallax, and fractional mass.

For Wolf 1062, the first two quantities have been determined to better than 1% from the data presented here, and are given in Table 3. The parallax listed in the Yale parallax catalog (van Altena, Lee, & Hoffleit 1995) is  $0^{\circ}.0998 \pm 0^{\circ}.0024$ , and is based upon six ground-based determinations. The *Hipparcos* parallax,  $0^{\circ}.09856 \pm 0^{\circ}.00266$  (ESA 1997), is in excellent agreement with the ground-based value, although slightly less precise. For the remainder of the present discussion, we adopt the formal weighted mean of the seven available independent measurements (six from the ground, one from *Hipparcos*):  $0.09919 \pm 0.00180$ .

To estimate the fractional mass of the secondary, we rely upon knowledge of the infrared properties of the components. The combination of the  $K$  magnitude for the system ( $K = 6.31 \pm 0.03$ ), the magnitude difference at  $K$  ( $1.4 \pm 0.1$  mag), and the parallax ( $0.09919 \pm 0.00180$ ) yields  $M_K$  for each component. The infrared MLR of Henry & McCarthy (1993, eqs. [2b] and [2c]) then allows us to make *photometric* mass estimates for the components:  $M_A = 0.349 \pm 0.010 M_{\odot}$  and  $M_B = 0.163 \pm 0.006 M_{\odot}$ . For the present purposes, we are interested in the fractional mass of the secondary rather than the individual mass values. The ratio of these masses can then be used to estimate the fractional mass of the secondary,  $f = M_B / (M_A + M_B) = 0.318 \pm 0.013$ . Ultimately, the fractional mass will be determined directly from the complete set of *HST* FGS3 position mode (POS) data, which will also provide a high-precision parallax with an expected error less than 1 mas.

Finally, using  $P$  and  $a$  from the *HST* FGS3 data and the weighted mean parallax, we find the total mass of the system to be  $0.543 \pm 0.031 M_{\odot}$ . From the estimate of the fractional mass,  $f$ , we find  $M_A = 0.370 \pm 0.022 M_{\odot}$  and  $M_B = 0.173 \pm 0.012 M_{\odot}$ , consistent with the masses estimated photometrically.

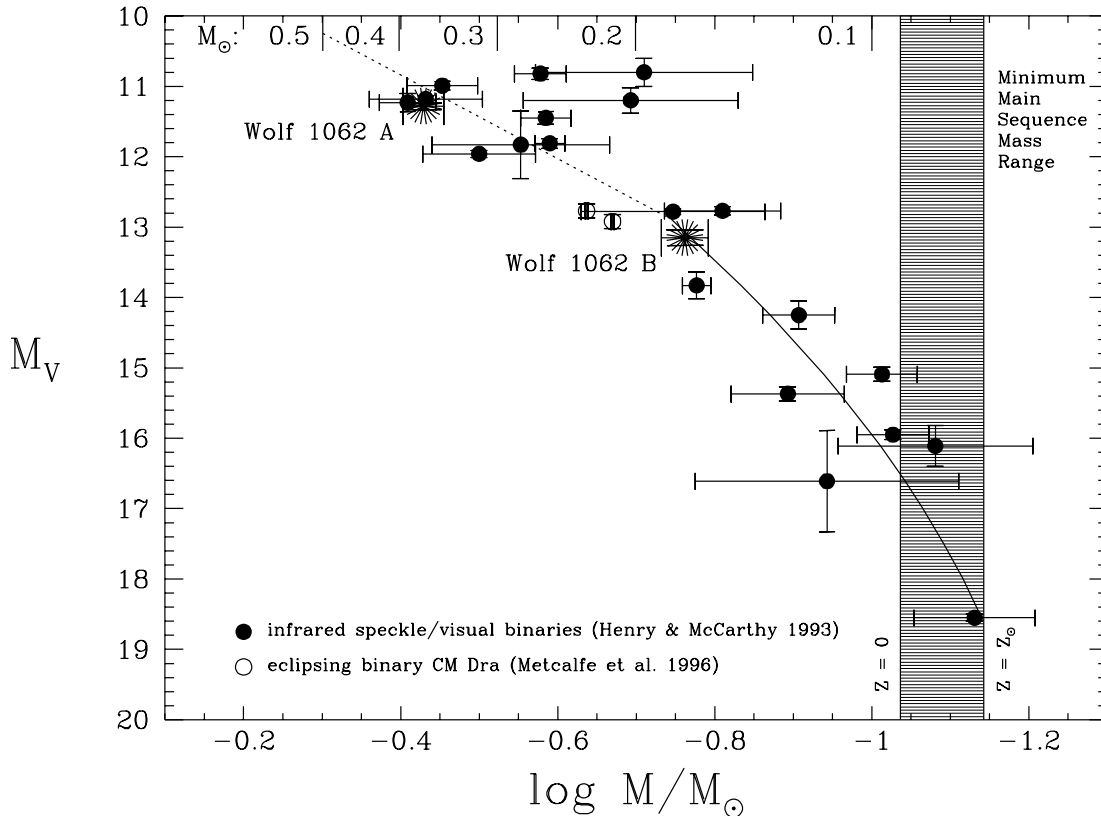


FIG. 4.—Mass-luminosity relation at  $M_V$  from Henry & McCarthy (1993) covering the range  $0.50 M_\odot$  to the end of the main sequence. Filled circles represent binaries resolved by infrared speckle and/or visual techniques. The open points represent the only eclipsing binary known to contain stars of such low mass. The fit to the data is discussed in their paper. The minimum main-sequence mass range is shaded, with the limits discussed in the text. The two components of the Wolf 1062 system are shown as stars. The masses of Wolf 1062A and B are estimates with appropriate error bars, because the fractional mass in the Wolf 1062 system has yet to be determined directly from *HST* FGS3 position-mode data.

#### 4.4. Mass-Luminosity Relation

In Figure 4 we show Wolf 1062A and B plotted with large stars on the MLR at  $M_V$  given in Henry & McCarthy (1993, Fig. 3). Only the portion below  $0.5 M_\odot$  is shown. Components of binaries resolved with infrared speckle and/or visual techniques are indicated by filled circles; no changes to these data have been made (except that the Gliese 508 system has been deleted, because it is now known to be triple). Adjustments to both the masses and magnitudes because of new values in the Yale parallax catalog, and because of *Hipparcos* parallaxes, as well as accurate measurements of the magnitude differences from our *HST* FGS3 program will be made and fully discussed in an upcoming paper (Henry et al. 1998). The improved mass determinations for the components in the eclipsing binary, CM Dra (represented by open points, Metcalfe et al. 1996) have been used ( $M_A = 0.2307 \pm 0.0010 M_\odot$  and  $M_B = 0.2136 \pm 0.0010 M_\odot$ ), with  $M_V$  values from Popper (1980;  $M_{V,A} = 12.77 \pm 0.10$  and  $M_{V,B} = 12.92 \pm 0.10$ ).

The minimum main-sequence mass range is shaded, with the limits assigned based upon the latest available models for low-mass stars and brown dwarfs. For zero metallicity, the minimum mass for stable hydrogen burning is  $0.092 M_\odot$  (Saumon et al. 1994), whereas for solar metallicity, the minimum mass is  $0.072 M_\odot$  (Chabrier & Baraffe 1997). Note that both Wolf 1062A and B fall near the empirical fit to the points on the MLR.

Shown in Figure 5 is the location of Wolf 1062B among

the lowest mass objects known in the MLR at  $M_K$ , also adapted from Henry & McCarthy (1993). This star is among only 11 known with dynamically determined masses less than  $0.20 M_\odot$ , and falls squarely on the empirical relation derived.

#### 5. CONCLUSIONS AND FUTURE EFFORTS

This work presents the first definitive binary star orbit determined entirely by the *Hubble Space Telescope*, and illustrates the power of Fine Guidance Sensor 3 for astrometric work. The target, Wolf 1062AB, has been resolved at 14 epochs into two low-mass red dwarf stars. The precision of the FGS3 measurements is 1–3 mas, even at separations as small as  $\sim 80$  mas, an unprecedented accuracy for such a faint system. The resulting masses, which currently rely upon an estimated fractional mass, have been derived to 6%. The secondary has a mass of only  $0.17 M_\odot$ , placing it among the 11 lowest mass objects for which accurate masses have been determined. Addition of three observations of the system after *HST* SMOV2, and a combined analysis of all TRANS and POS data, will provide a parallax and directly determined fractional mass, and ultimately lead to even better masses for Wolf 1062A and B. We will continue to use FGS3 for future observations on additional multiple systems through Cycle 8, after which we anticipate that the new FGS1R will be used to map out the mass-luminosity relation at the bottom of the stellar main sequence.

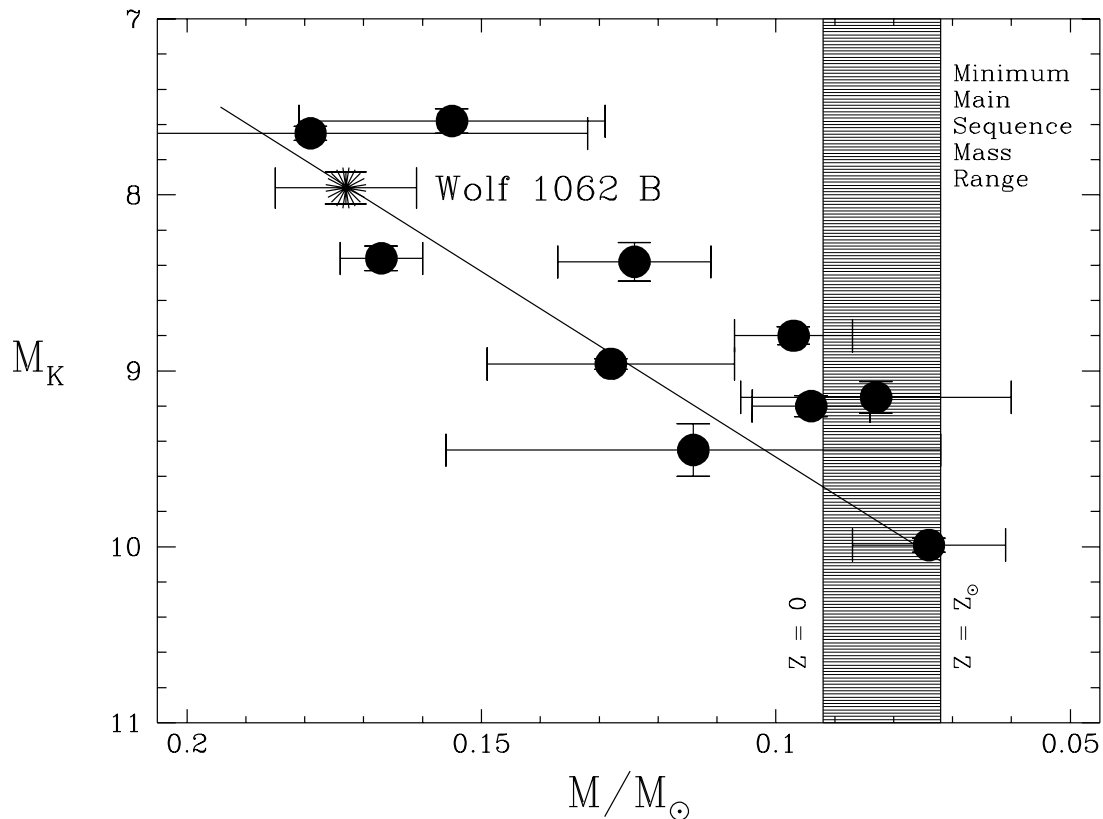


FIG. 5.—Mass-luminosity relation at  $M_K$  from Henry & McCarthy (1993), near the end of the main sequence. Filled circles represent binaries resolved by infrared speckle and/or visual techniques. The fit to the data is discussed in their paper. The minimum main-sequence mass range is shaded, with the limits discussed in the text. Wolf 1062B is represented by the star, and is only the eleventh point with a dynamically determined mass less than  $0.20 M_\odot$ . The mass of Wolf 1062B is an estimate with appropriate error bars, because the fractional mass in the Wolf 1062 system has yet to be determined directly from *HST* FGS3 position mode data.

We thank Denise Taylor and Jack McConnell for their tireless efforts that made this *HST* observational program possible. Support for this work was provided by NASA through grant number GO-06047.03-94A from the Space Telescope Science Institute, which is operated by the Association of Universities for Research in Astronomy, Inc.,

under NASA contract NAS 5-26555. T. J. H. received additional support from NASA through Hubble Fellowship grant HF-1058.01-94A, also from STScI. Support for this work was also provided by NASA under grant NAG 5-1603 to the University of Texas.

#### REFERENCES

- Benedict, G. F., et al. 1994, *PASP*, 106, 327  
 Chabrier, G., & Baraffe, I. 1997, *A&A*, 327, 1039  
 ESA. 1997, *The Hipparcos and Tycho Catalogues* (ESA SP-1200) (Noordwijk: ESA)  
 Franz, O. G., Wasserman, L. H., Nelan, E., Lattanzi, M. G., Bucciarelli, B., & Taff, L. G. 1992, *AJ*, 103, 190  
 Franz, O. G., et al. 1991, *ApJ*, 377, L17  
 ———, 1994, *BAAS*, 185, No. 85.24  
 ———, 1995, *BAAS*, 187, No. 43.06  
 Harrington, R. S. 1977, *PASP*, 89, 214  
 Hartkopf, W. I. 1992, in *IAU Colloq. 135, Complementary Approaches to Double and Multiple Star Research*, ed. H. A. McAlister & W. I. Hartkopf (ASP Conf. Ser. 32) (San Francisco: ASP), 459  
 Henry, T. J., & McCarthy, D. W., Jr. 1993, *AJ*, 106, 773  
 Henry, T. J., Franz, O. G., Wasserman, L. H., Benedict, G. F., Shelus, P. J., Ianna, P. A., Kirkpatrick, J. D., & McCarthy, D. W. 1998, *ApJ*, submitted  
 Holfeltz, S. T., ed. 1996, *Fine Guidance Sensor Instrument Handbook* (version 6.0; Baltimore: STScI)  
 Kirkpatrick, J. D., Henry, T. J., & McCarthy, D. W., Jr. 1991, *ApJS*, 77, 417  
 Leggett, S. K. 1992, *ApJS*, 82, 351  
 Liebert, J., & Probst, R. G. 1987, *ARA&A*, 25, 473  
 Lippincott, S. L. 1977, *AJ*, 82, 925  
 McCarthy, Jr., D. W. 1986, in *Astrophysics of Brown Dwarfs*, ed. M. C. Kafatos, R. S. Harrington, & S. P. Maran (Cambridge: Cambridge Univ. Press), 9  
 Metcalfe, T. S., Mathieu, R. D., Latham, D. W., & Torres, G. 1996, *ApJ*, 456, 356  
 Popper, D. M. 1980, *ARA&A*, 18, 115  
 Saumon, D., Bergeron, P., Lunine, J. I., Hubbard, W. B., & Burrows, A. 1994, *ApJ*, 424, 333  
 van Altena, W. F., Lee, J. T., & Hoffleit, E. D. 1995, *The General Catalogue of Trigonometric Stellar Parallaxes, Vols. 1 and 2* (4th ed.; New Haven: Yale Univ. Obs.)  
 Weis, E. W. 1996, *AJ*, 112, 2300